High-speed 32×32 MEMS optical phased array

Mischa Megens[a], Byung-Wook Yoo[b], Trevor Chan[a], Weijian Yang[b], Tianbo Sun[b],
Connie J. Chang-Hasnain[b], Ming C. Wu[b], and David A. Horsley[a,1]
[a]Mechanical and Aerospace Engineering, University of California, Davis, CA USA 95616
[b]Electrical Engineering and Computer Sciences, University of California, Berkeley, CA USA 94720

ABSTRACT

Optical phased arrays (OPAs) with fast response time are of great interest for various applications such as displays, free space optical communications, and lidar. Existing liquid crystal OPAs have millisecond response time and small beam steering angle. Here, we report on a novel 32×32 MEMS OPA with fast response time (<4 microseconds), large field of view (±2°), and narrow beam divergence (0.1°). The OPA is composed of high-contrast grating (HCG) mirrors which function as phase shifters. Relative to beam steering systems based on a single rotating MEMS mirror, which are typically limited to bandwidths below 50 kHz, the MEMS OPA described here has the advantage of greatly reduced mass and therefore achieves a bandwidth over 500 kHz. The OPA is fabricated using deep UV lithography to create submicron mechanical springs and electrical interconnects, enabling a high (85%) fill-factor. Each HCG mirror is composed of only a single layer of polysilicon and achieves >99% reflectivity through the use of a subwavelength grating patterned into the mirror's polysilicon surface. Conventional metal-coated MEMS mirrors must be thick (1-50 μm) to prevent warpage arising from thermal and residual stress. The single material construction used here results in a high degree of flatness even in a thin 400 nm HCG mirror. Beam steering is demonstrated using binary phase patterns and is accomplished with the help of a closed-loop phase control system based on a phase-shifting interferometer that provides in-situ measurement of the phase shift of each mirror in the array.

Keywords: optical phased arrays, beam steering, micro electromechanical systems, high contrast gratings.

1. INTRODUCTION

Optical phased arrays (OPAs)[1, 2] are versatile beam steering devices suitable for a variety of applications including LIDAR, free-space optical communication, 3D holographic displays, and high-resolution 3D imaging.[3, 4] An OPA consists of a two-dimensional (2D) array of phase shifters which impose a desired phase profile on an incoming beam of light. Unlike mirror-based beam steering systems, an OPA can be programmed to generate multiple, simultaneously-scanning beams in the OPA's field of view, allowing precise pointing and tracking of multiple targets. OPA's also offer fast random-access pointing and dynamic focusing/defocusing capabilities. An OPA is usually much faster than a single steering mirror as individual phase shifters are much smaller and more nimble than a large scanning mirror.

The dominant OPA technology is based on liquid crystal phase shifters, which have been studied extensively since their initial demonstration using liquid crystal television panels.[5, 6] However, liquid crystals have limited operating speed because it takes tens of milliseconds for an electric field to reorient the molecules of the liquid crystal. Liquid crystals also suffer from the disadvantage that, as a continuous medium, sharp phase transitions (e.g. in the region where the phase pattern wraps from 2π to 0 radians) are not properly expressed. In addition, liquid crystal materials tend to be highly temperature sensitive, necessitating active temperature regulation in many applications.

More recently, micro-electromechanical systems (MEMS) have been used to produce OPAs.[7, 8] A typical MEMS-based phase shifter is realized by a "piston" mirror which is displaced to provide the desired phase shift. Conventional MEMS mirrors are made of metal-coated single-crystal or polycrystalline silicon, or multi-layer distributed Bragg reflectors (DBRs). Though faster than bulk mirrors, the mass of such multi-layer mirrors still limits the operating speed of MEMS-based OPAs. Moreover, thin-film mirrors composed of dissimilar materials suffer from temperature sensitivity due to differences in the coefficient of thermal expansion (CTE) of the various layers. This CTE mismatch often causes mirrors

[1] dahorsley@ucdavis.edu, phone: 1-530-341-3236, fax: 1-530-752-4158

MOEMS and Miniaturized Systems XIII, edited by Wibool Piyawattanametha,
Yong-Hwa Park, Proc. of SPIE Vol. 8977, 89770H · © 2014 SPIE
CCC code: 0277-786X/14/$18 · doi: 10.1117/12.2044197

to warp, degrading optical performance. The residual absorption in the metal reflector also limits the maximum optical power before catastrophic damage occurs.

In this paper, we demonstrate an ultrafast MEMS OPA composed of a 32×32 array of lightweight high-contrast-grating (HCG) mirrors. The HCG mirror consists of a single, thin 400 nm layer of polysilicon that is patterned into a sub-wavelength diffraction grating. Unlike earlier multi-layer MEMS mirrors, the HCG is made of a single dielectric layer, achieving high reflectivity (~99.9%) over a broad optical bandwidth.[9, 10] The HCG's single-material construction results in greater manufacturability since residual stress is easily controlled when depositing the single polysilicon layer and the process eliminates the need for non-CMOS compatible metals such as gold. The HCG-OPA has the potential to operate at high optical power without warping due to CTE mismatch and without the thermal damage that plagues mirrors composed of low melting-point metals (e.g. Au and Al). The mass of a 20×20 μm^2 HCG mirror is 140 pg, about ~100× lighter than a DBR of comparable reflectivity. Since the mirror's maximum acceleration increases by the same factor as the mass reduction, this low mass increases the maximum operating bandwidth of the HCG OPA.

2. SYSTEM DESIGN

The complete beam steering system, illustrated in Figure 1, is composed of a laser source, MEMS OPA, and phase-monitoring interferometer. Polarized light from the source is directed towards the OPA, with a small (1%) fraction of the light split into the interferometer to provide in-situ monitoring of the phase of each pixel in the array.[11] This phase monitoring system can be used to calibrate the phase-voltage characteristics of the OPA and to provide slow correction of phase offsets (arising from e.g. thermal shifts within the system), however the beam steering results presented here were collected using open-loop voltage control without correction for phase variations across the OPA. The steerable beam exiting the system passes through a lens pair with focal lengths f_1 and f_2, providing an angle magnification of f_1/f_2 which was set to 5 in experiments presented here.

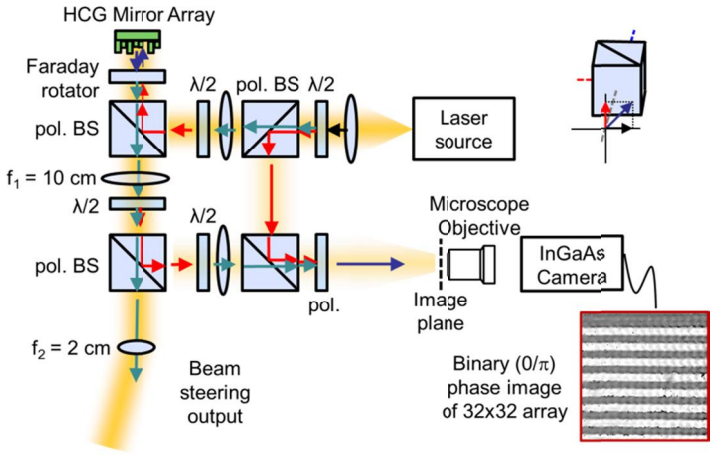

Figure 1. Beam steering system block diagram. Light from the laser source is collimated and directed at the MEMS OPA through a polarizing beamsplitter (pol. BS). Half-wave plates (λ/2) are used to rotate the polarization and two additional polarizing beamsplitters are used to tap a fraction of the light into an interferometer that provides in-situ monitoring of the phase of each mirror in the OPA. A lens pair is used to amplify the beam steering angle at the final aperture.

In phased-array beam steering, the discrete OPA mirrors are assigned phase settings that approximate the desired continuous phase profile, modulo 2π, as illustrated in Figure 2. In a reflective OPA, the phase shift corresponds to twice the mirror displacement, so 775 nm displacement corresponds to 2π phase shift at the nominal operating wavelength $\lambda = 1550$ nm. The maximum beam steering angle that can be achieved before the magnification optics is $\theta = \pm\sin(\lambda/2\Lambda) = \pm 2°$, where $\Lambda = 22$ μm is the mirror pitch.

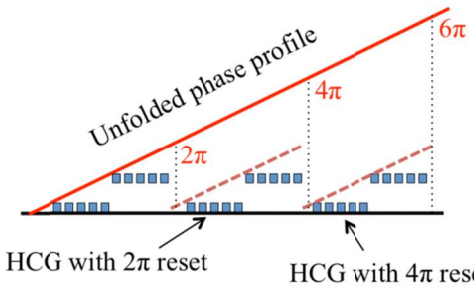

Figure 2. Illustration of phased-array beam steering at the maximum steering angle. The phase of each HCG mirror is set to approximate the desired phase pattern modulo 2π.

The 32×32 OPA is composed of 20×20 μm^2 polysilicon HCG mirrors that are defined in a 400 nm thick polysilicon layer using a deep ultraviolet (DUV) lithography system (ASML 5500/300 DUV Stepper) capable of resolving 250 nm features. The polysilicon layer is polished using chemical-mechanical polishing (CMP) before lithography to produce a smooth surface for lithography, thereby reducing edge roughness in the patterned grating bars and ensuring a smooth surface in the final HCG. The complete fabrication process was described earlier.[12, 13] Scanning electron micrograph (SEM) images, Figure 3, show that each mirror consists of a grating with 1250 nm period and 570 nm bar width supported at four corners by 300 nm wide, 18 μm long flexure springs. The flexures are mechanically connected to the silicon substrate through electrically-insulating Si_3N_4 anchors. An 85% fill factor is achieved by minimizing the space between the 20 μm mirrors: as illustrated in the SEM images, this 2 μm space contains two 300 nm flexure springs and two anchors, demonstrating the need for submicron lithography.

The mirrors are electrostatically actuated by applying a voltage between the polysilicon mirror layer and the silicon substrate, which serves as a common ground electrode for the entire OPA. In the first prototype OPA reported here, the 32 mirrors in each of the 32 columns are electrically connected together. Each column is driven at up to 45V using a custom 32-channel digital-to-analog converter board. One-dimensional beam steering is demonstrated by actuating the mirrors in each column together.

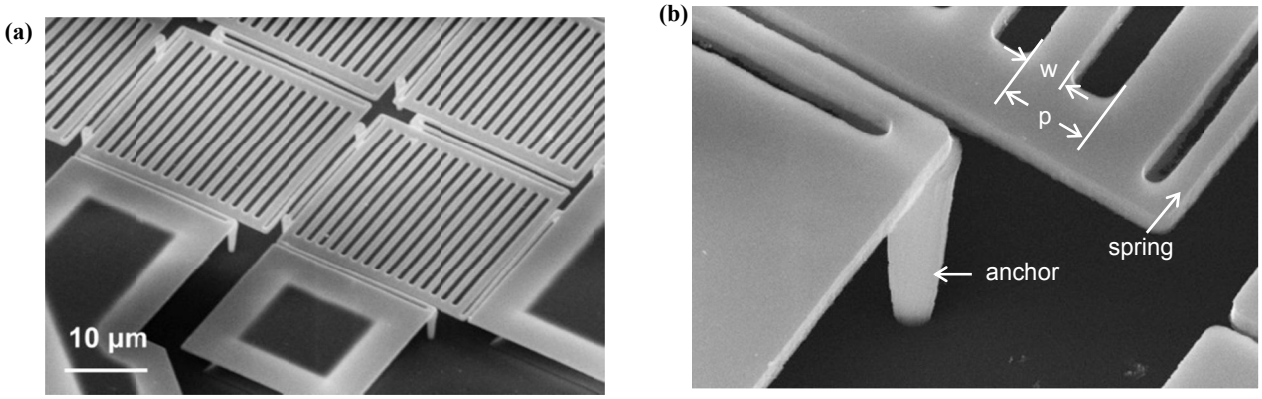

Figure 3. SEM images of the OPA showing individual 20×20 μm^2 HCG mirrors. (a) Each HCG is supported by flexure springs at the mirror's four corners, resulting in 22 μm pitch between mirrors. The low-stress polysilicon layer is extremely flat, resulting in near-zero distortion across the surface of the array. The 400 nm thick polysilicon mirrors are released by etching a sacrificial SiO_2 layer beneath the polysilicon layer: SiO_2 remains in the dark regions beneath the polysilicon interconnect. (b) A close-up of the corner of one mirror showing the grating's 570 nm bar width (w) and 1250 nm period (p). Each flexure spring is mechanically connected to the Si substrate through a cylindrical Si_3N_4 insulated anchor.

The high contrast grating (HCG) is a sub-wavelength diffraction grating that achieves high reflectivity over a broad range of wavelengths. Designed with a grating period (p) in the near-wavelength regime (i.e. $\lambda/n_r < p < \lambda/n_a$, where n_r and n_a are the refractive indices of the grating bars and air, respectively), HCG's can achieve high reflectivity (~99.9%) and high quality-factor optical resonances ($Q > 10^7$).[14] Here, the HCG period and bar width were designed using finite difference time domain (FDTD) analysis to achieve high reflectivity at a center wavelength $\lambda = 1550$ nm. A contour map of the simulated reflectivity for transverse electric (TE) polarized light as a function of grating period and bar width is

shown in Figure 4. Because the bar and space widths are on the order of 500 nm, manufacturing variations on the order of a few 10's of nm are expected and the grating must be designed with these tolerances in mind. The final design, 1250 nm period and 570 nm bar width, achieves 99.9% reflectivity and maintains > 99% reflectivity over ±35 nm width variations. Notably, the HCG is a broadband reflector: the nominal grating design achieves 99.9% reflectivity from 1548 nm to 1575 nm and higher than 99% reflectivity from 1517 nm to 1605 nm.

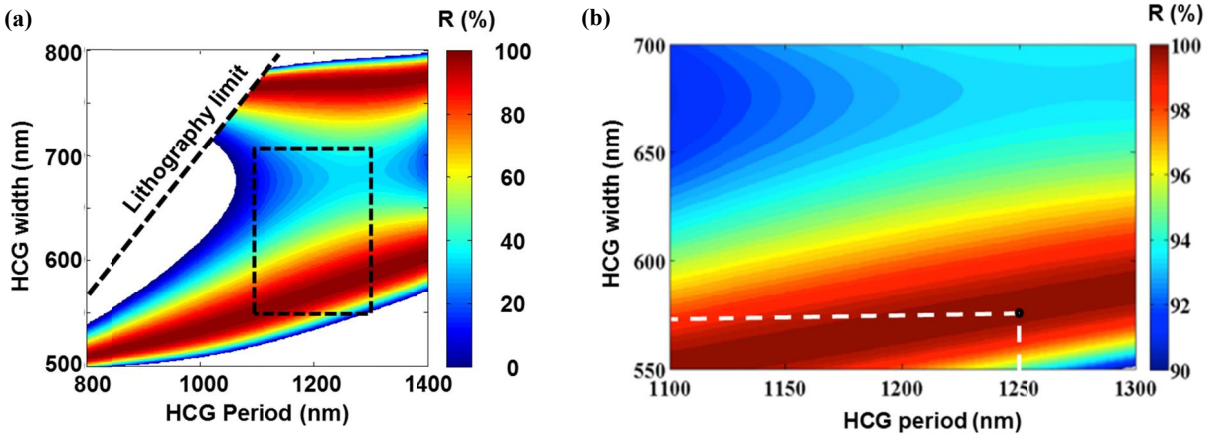

Figure 4. FDTD simulations of HCG mirror reflectivity as a function of bar width and period for a 400 nm thick polysilicon layer at λ = 1550 nm. (a) Reflectivity over the range of possible dimensions showing the 250 nm lithography resolution limit. (b) Close-up of the region surrounding the selected width and period which are indicated with a black dot. The reflectivity is greater than 99% for dimensional variations up to ±35 nm around the nominal design.

3. RESULTS AND DISCUSSION

The actuation of individual HCG mirrors was characterized using static and dynamic voltage inputs. The quasi-static displacement response of a typical mirror, measured using phase-shifting interferometry, is shown in Figure 5(a). The actuation response displays the characteristic voltage-squared dependence expected from electrostatic actuation, with a maximum phase shift of 1.7π occurring at 38 V. The mirror frequency response, measured using a laser Doppler vibrometer and shown in Figure 5(b), displays a 0.46 MHz resonant frequency, in good agreement with finite element method (FEM) models for the 400 nm thick polysilicon mirror. Time-response measurements show that the mirror's response is well-approximated as an underdamped harmonic oscillator with a damping ratio ζ = 0.2 and a damped natural frequency of 0.46 MHz. The 10% settling time in response to a step voltage input is 3.8 μs.[13]

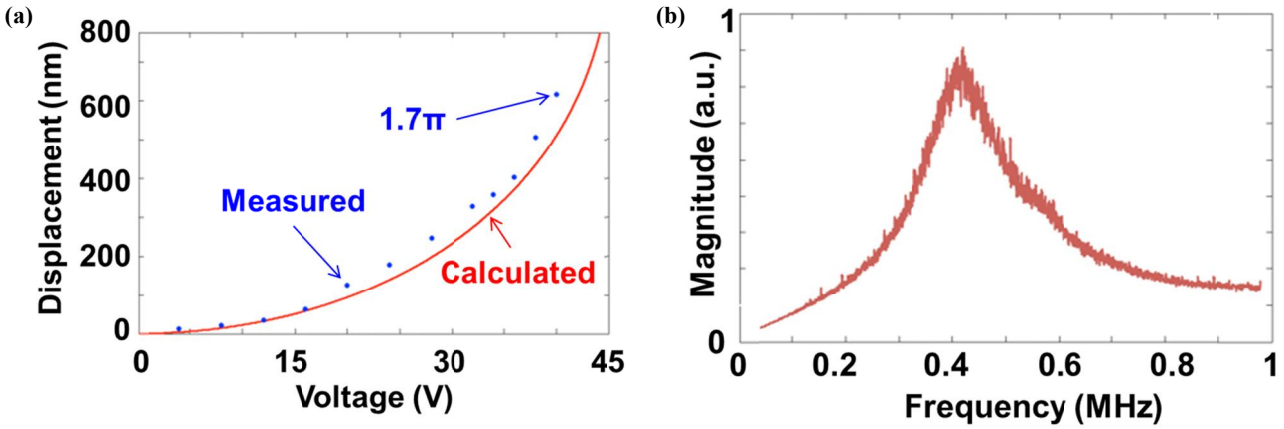

Figure 5. Electrostatic actuation of HCG mirrors. (a) Quasi-static voltage-displacement characteristic showing measured displacements (points) and a theoretical fit (line). A maximum phase shift of 1.7π radians is achieved. (b) Frequency response measured via LDV showing a resonance peak at 0.46 MHz.

Beam steering experiments were conducted using binary phase patterns in which the HCG mirror's phase was set to either 0 or π radians. The voltage required to achieve a phase shift of π radians was first determined using interferometry to measure the phase-voltage characteristic of the mirrors in the array. The nominal voltage required, 34 V, was found to vary by approximately ±1 V across the array. For simplicity, the same voltage was used for all the mirrors in the array in beam steering experiments, resulting in small phase errors across the OPA. These phase errors are small (on the order of ±0.2 radians) due to the relatively shallow slope of the phase-voltage characteristic, Figure 5(b). Phase images of the OPA with mirrors in the on (π radians) and off state (0 radians), measured via interferometry and shown in Figure 6, illustrate the uniformity of the phase across the array.

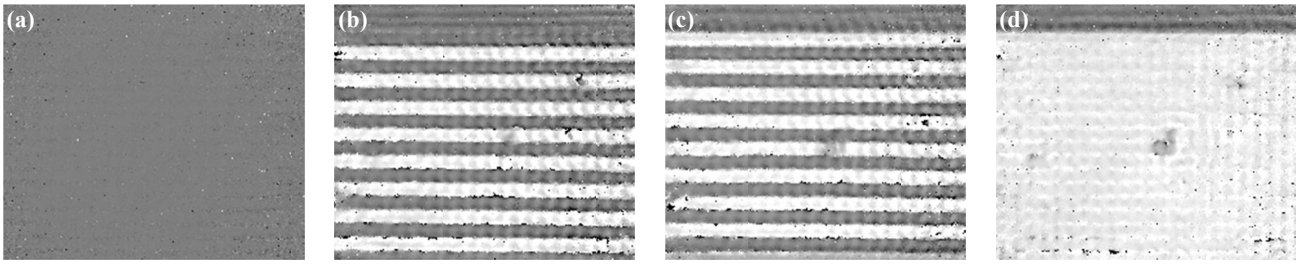

Figure 6. Phase images of 16 columns of the 32x32 OPA measured via interferometry: (a) all mirrors off; (b) π phase shift applied to even columns, odd columns off; (c) π phase shift applied to odd columns, even columns off; (d) π phase shift applied to all columns.

The phase patterns used for beam steering are illustrated in Figure 7(a) and the resulting far-field beam steering images are shown in Figure 7(b). With a binary pattern, normally-incident light is diffracted symmetrically about the 0^{th} order beam, with θ_1, the angle of the 1^{st} diffraction order, increasing as the number of mirrors in each phase period is reduced. State 0 corresponds to the rest position of the mirrors, with all the power in the 0^{th} order beam, while States 1-3 correspond to 8, 4, and 2 mirrors per phase period, resulting in diffraction angle $\theta_1 = 0.5°$, 1.0°, and 2.0°, respectively.

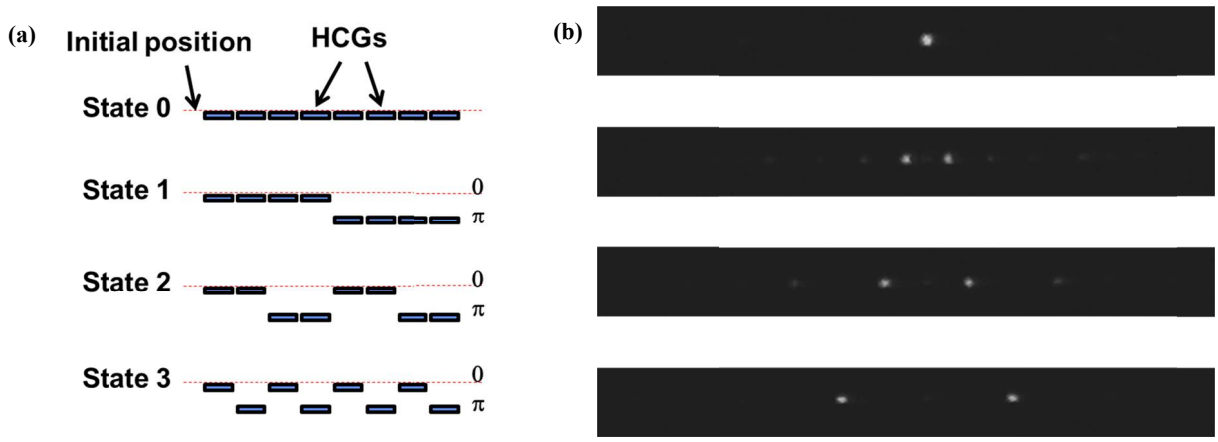

Figure 7. Beam steering using binary phase patterns: (a) phase patterns; (b) far-field images for each state.

The diffracted intensity was studied as a function of phase shift φ applied to the mirrors at the maximum steering angle (State 3 in Figure 7(b)). The intensity in the 1^{st} order diffraction lobe at the maximum angle is given by[15] $I=I_{max}\,sin^2(\varphi/2)$, where the maximum intensity I_{max} occurs at $\varphi = \pi$. The measured intensity versus the theoretical intensity is shown in Figure 8, showing good agreement between theory and experiment.

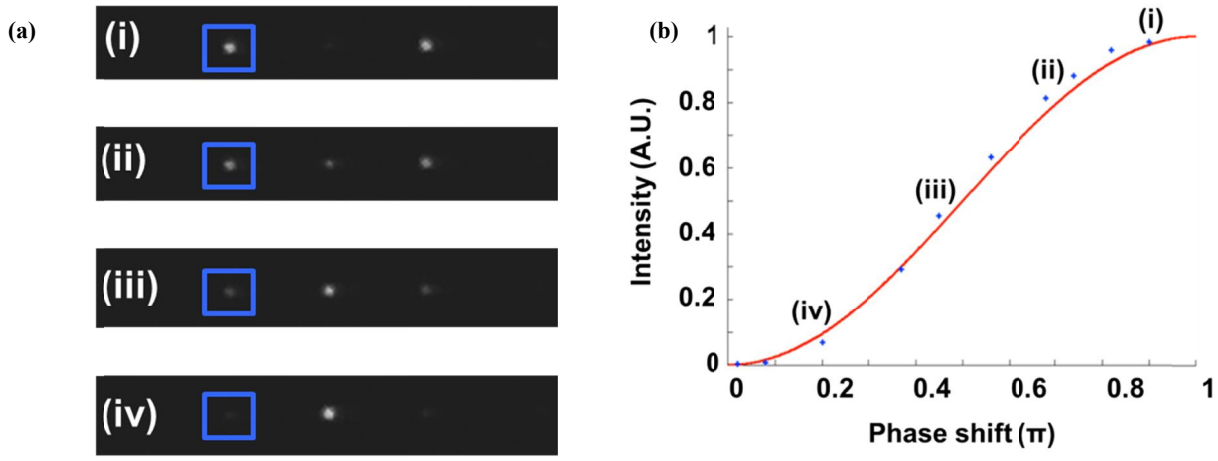

Figure 8. Diffraction efficiency versus phase shift for binary phase patterns. (a) Far-field images showing the intensity in the 0^{th} and 1^{st} diffraction orders (indicated with a blue square) as the maximum phase shift in the binary pattern is decreased from π (i) to 0.2 π (iv). (b) Plot of measured intensity in the 1^{st} diffraction orders (points) along with the theoretical diffraction efficiency of a binary phase grating (line) versus phase shift. At π radians phase shift, the reflected intensity is almost entirely in the 1^{st} diffraction orders; the diffracted intensity diminishes and the intensity in the 0^{th} order beam increases as the binary pattern's phase shift is reduced.

4. CONCLUSIONS

A novel micro-electromechanical systems (MEMS) optical phased array with high fill-factor has been successfully developed for fast beam steering. The 32×32 array is comprised of sub-wavelength high-contrast-grating (HCG) reflectors made of polysilicon. Each HCG mirror is 20×20 μm^2, and the spacing between mirrors is 2 μm, resulting in 85% fill-factor. The thickness, width and period of the HCG grating bars are 400 nm, 570 nm and 1250 nm, respectively, resulting in a simulated ~99.9% reflectivity. Each HCG is vertically driven by electrostatic force to create a voltage-controlled phase shift and coherent interference in the far field patterns. The measured maximum beam steering angle is ±2.0°. The average resonant frequency of the array is 0.46 MHz, allowing for fast beam steering. The MEMS HCG optical phased array is a scalable two-dimensional platform capable of more versatile beam steering applications requiring better resolution than currently available OPAs.

ACKNOWLEDGEMENTS

This work was supported by the DARPA SWEEPER program (Grant No. HR0011-10-2-0002). Devices were fabricated at the Marvell Nanofabrication Laboratory at UC Berkeley.

REFERENCES

[1] Sun, J., Timurdogan, E., Yaacobi, A., Hosseini, E. S., and Watts, M. R., "Large-scale nanophotonic phased array," Nature 493(7431), 195-199 (2013).

[2] McManamon, P. F., Bos, P. J., Escuti, M. J., Heikenfeld, J., Serati, S., Xie, H., and Watson, E. A., "A Review of Phased Array Steering for Narrow-Band Electrooptical Systems," Proceedings of the IEEE 97(6), 1078-1096 (2009).

[3] Doylend, J. K., Heck, M. J. R., Bovington, J. T., Peters, J. D., Coldren, L. A., and Bowers, J. E., "Two-dimensional free-space beam steering with an optical phased array on silicon-on-insulator," Optics Express 19(22), 21595-21604 (2011).

[4] McManamon, P. F., Dorschner, T. A., Corkum, D. L., Friedman, L. J., Hobbs, D. S., Holz, M., Liberman, S., Nguyen, H. Q., Resler, D. P., Sharp, R. C., and Watson, E. A., "Optical phased array technology," Proceedings of the IEEE 84(2), 268-298 (1996).

[5] Engstrom, D., O'Callaghan, M. J., Walker, C., and Handschy, M. A., "Fast beam steering with a ferroelectric-liquid-crystal optical phased array," Applied Optics 48(9), 1721-1726 (2009).
[6] Jau, H. C., Lin, T. H., Fung, R. X., Huang, S. Y., Liu, J. H., and Fuh, A. Y. G., "Optically-tunable beam steering grating based n azobenzene doped cholesteric liquid crystal," Optics Express 18(16), 17498-17503 (2010).
[7] Bifano, T. G., Perreault, J., Mali, R. K., and Horenstein, M. N., "Microelectromechanical deformable mirrors," IEEE Journal of Selected Topics in Quantum Electronics 5(1), 83-89 (1999).
[8] Krishnamoorthy, U., Li, K., Yu, K., Lee, D., Heritage, J. P., and Solgaard, O., "Dual-mode micromirrors for optical phased array applications," Sensors and Actuators A-Physical 97-8, 21-26 (2002).
[9] Huang, M. C. Y., Zhou, Y., and Chang-Hasnain, C. J., "A surface-emitting laser incorporating a high-index-contrast subwavelength grating," Nature Photonics 1(2), 119-122 (2007).
[10] Yoo, B. W., Megens, M., Chan, T., Sun, T., Yang, W., Chang-Hasnain, C. J., Horsley, D. A., and Wu, M. C., "Optical phased array using high contrast gratings for two dimensional beamforming and beamsteering," Optics Express 21(10), 12238-12248 (2013).
[11] Chan, T. K., Megens, M., Yoo, B. W., Wyrwas, J., Chang-Hasnain, C. J., Wu, M. C., and Horsley, D. A., "Optical beamsteering using an 8 × 8 MEMS phased array with closed-loop interferometric phase control," Optics Express 21(3), 2807-2815 (2013).
[12] Yoo, B. W., Megens, M., Chan, T. K., Sun, T., Yang, W., Horsley, D. A., Chang-Hasnain, C. J., and Wu, M. C., "32x32 Optical phased array with ultra-lightweight high-contrast-grating mirrors," Proc. 17th Intl. Conf. on Solid-State Sensors Actuators and Microsystems 2505-2508 (2013).
[13] Yoo, B. W., Megens, M., Sun, T., Yang, W., Chang-Hasnain, C. J., Horsley, D. A., and Wu, M. C., "32×32 optical phased array using polysilicon sub-wavelength high-contrast-grating mirrors," Optics Express, submitted (2014).
[14] Karagodsky, V., and Chang-Hasnain, C. J., "Physics of near-wavelength high contrast gratings," Optics Express 20(10), 10888-10895 (2012).
[15] Amm, D. T., and Corrigan, R. W., "Grating Light Valve™ Technology: Update and Novel Applications," SID Symposium Digest of Technical Papers 29(1), 29-32 (1998).